DOI: 10.1002/anie.200905947

Molecular Rotors

A Molecular Double Ball Bearing: An Ag^{I}–Pt^{II} Dodecanuclear Quadruple-Decker Complex with Three Rotors**

Shuichi Hiraoka,* Yoshihiro Hisanaga, Motoo Shiro, and Mitsuhiko Shionoya*

Metal complexes with dynamic properties[1] arising from multipoint ligand exchanges around coordination environments are up-and-coming molecules for next-generation molecular machines.[2] We previously described a supramolecular ball bearing, $[Ag_3\mathbf{1}{\cdot}\mathbf{2}]^{3+}$, in which two different hexasubstituted benzene molecules, **1** and **2**, can rotate relative to each other on three Ag^{I} ions located between them (Figure 1 a).[3] The rotational motion of the two rotor parts in the trinuclear helical complex takes place through intramolecular ligand exchange and flip motion (Figure 1 e), both of which are accompanied by the inversion of the helical structure, as revealed by a variable-temperature (VT) ^{1}H NMR spectroscopic study of the molecular ball bearings formed from chiral trismonodentate ligands.[3b] More recently, with a view towards the long-range transmission of rotational motions in molecular-machinery systems, we developed molecular rotor–transmitter–rotors, $[Ag_6M_3\mathbf{1}_2{\cdot}\mathbf{3}_2]^{(3n+6)+}$ ($M = Ag^{I}$ ($n=1$) or Hg^{II} ($n=2$)), in which the motions of the two terminal rotors, **1**, are strongly correlated with each other through the helix inversion of a central supramolecular transmitter, $[M_3\mathbf{3}_2]^{3n+}$, located between the two rotors (Figure 1 b).[4] The crystal structure of a quadruple-decker silver nonanuclear complex, $[Ag_9\mathbf{1}_2{\cdot}\mathbf{3}_2{\cdot}(TfO)_9]$ (TfO^-: $CF_3SO_3^-$), indicated that the complex has a helical structure, and that the four ligands are mechanically interlocked with one another (Figure 3 c). A VT ^{1}H NMR spectroscopic study revealed that the rates of helix inversion in the two rotors, **1**, and the transmitter, $[Ag_3\mathbf{3}_2]^{3+}$, were identical, although the rate was slower than that observed for a simple molecular ball bearing. Thus, although the two terminal rotors **1** are 1.5 nm apart, the motions of the two rotors are strongly correlated through the central supramolecular transmitter $[Ag_3\mathbf{3}_2]^{3+}$.

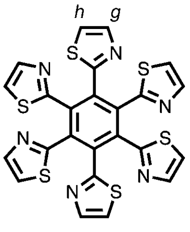

1

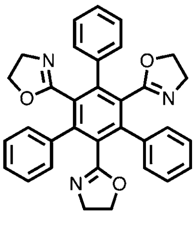

2

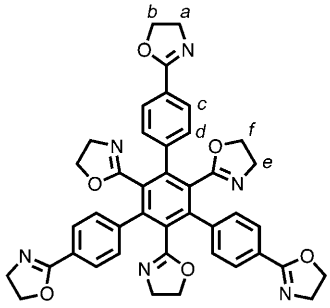

3

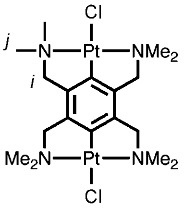

$\boldsymbol{Pt}Cl_2$

In view of the interlocked structure found in the molecular rotor–transmitter–rotors, their rotational rates and the correlation in motion between the two rotors should vary depending on the structural elements of the transmitter. For example, if the two ligands **3** of the transmitter are connected by different metal ions or complexes, we thought it should be possible to control the structural and functional correlation of the two terminal rotors by adjusting the degree of structural interlocking of the connecting parts.

Herein, we report the design of a novel transmitter, $[\boldsymbol{Pt}_3\mathbf{3}_2]^{6+}$, through the replacement of the central three Ag^{I} (or Hg^{II}) ions of $[Ag_3\mathbf{3}_2]^{3+}$ (or $[Hg_3\mathbf{3}_2]^{3+}$) with three 7 Å long dinuclear Pt^{II} pincer complexes, $\boldsymbol{Pt}^{2+}$ (Figure 1 d). Since the two ligands **3** can not interact directly with each other within the sandwich-shaped Pt^{II}-mediated transmitter $[\boldsymbol{Pt}_3\mathbf{3}_2]^{6+}$, the "interlocking" of their motions could only occur through the connecting parts. Therefore, it is extremely useful for the development of long-range motion transmitters or multiple ball bearings to examine the degree of structural interlocking and helix inversion within the central transmitter. A VT ^{1}H NMR spectroscopic study of the $[Ag_6\boldsymbol{Pt}_3\mathbf{1}_2{\cdot}\mathbf{3}_2]^{12+}$ complex indicated that the rate of rotation of the two terminal rotors in the complex is faster than that in $[Ag_9\mathbf{1}_2{\cdot}\mathbf{3}_2]^{9+}$, and that the helix inversions of the inner and outer oxazoline rings in **3** take place with different frequencies. Thus, the motional

---

[*] Dr. S. Hiraoka, Y. Hisanaga, Prof. Dr. M. Shionoya
Department of Chemistry, Graduate School of Science
The University of Tokyo
7-3-1 Hongo, Bunkyo-ku, Tokyo 113-0033 (Japan)
Fax: (+81) 3-5841-8061
E-mail: hiraoka@chem.s.u-tokyo.ac.jp
shionoya@chem.s.u-tokyo.ac.jp

Dr. S. Hiraoka
Precursory Research for Embryonic Science and Technology (PRESTO), Japan Science and Technology Agency
4-1-8 Honcho, Kawaguchi, Saitama 332-0012 (Japan)
Fax: (+81) 3-5841-1530

Dr. M. Shiro
Rigaku Corporation
3-9-12 Matsubaracho, Akishima, Tokyo 196-8666 (Japan)

[**] This research is supported by Grants-in-Aid from MEXT of Japan and the Global COE Program for Chemistry Innovation.

Supporting information for this article, including details of experimental procedures, is available on the WWW under http://dx.doi.org/10.1002/anie.200905947.

© 2010 Wiley-VCH Verlag GmbH & Co. KGaA, Weinheim

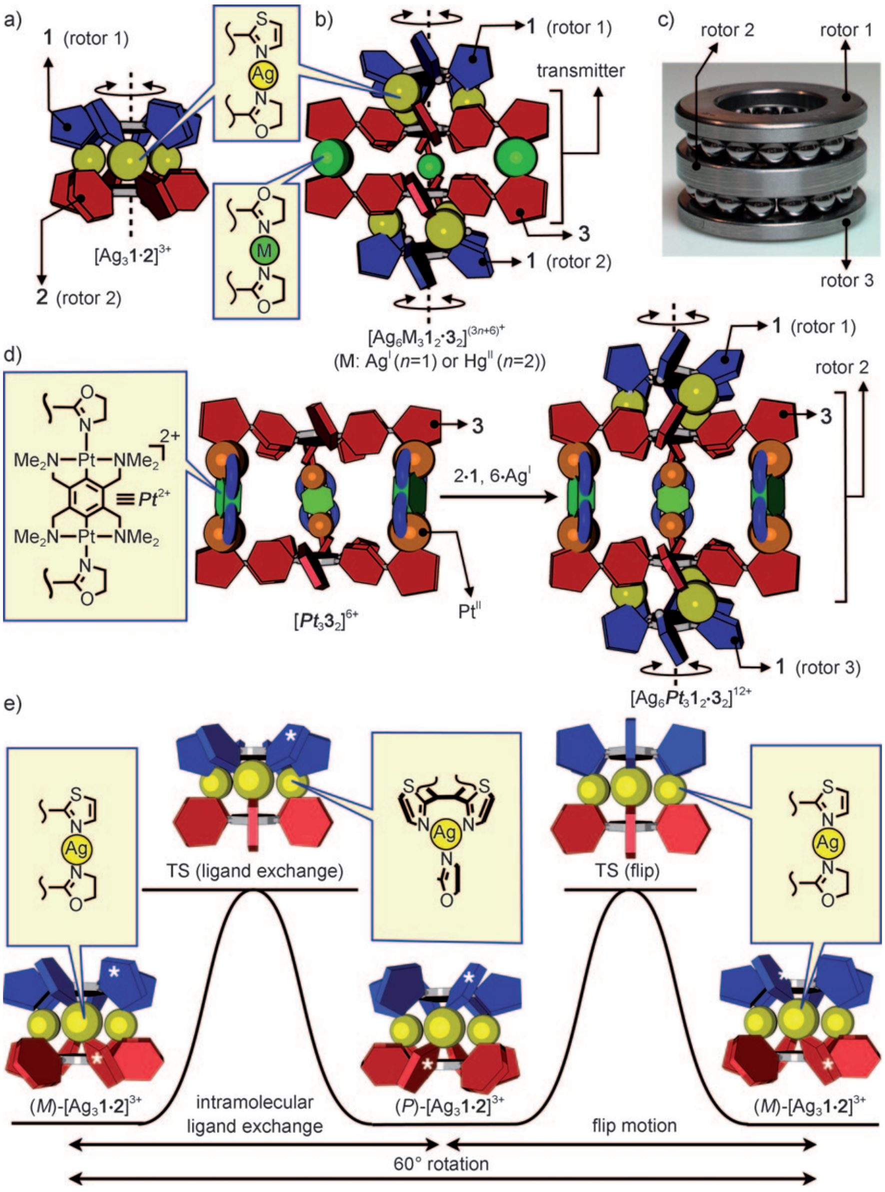

Figure 1. Schematic representation of a) a trinuclear molecular ball bearing and b) a nonanuclear rotor–transmitter–rotor. c) Photograph of a macroscopic double ball bearing. d) Synthetic strategy for the construction of a dodecanuclear Ag^I–Pt^{II} molecular double ball bearing. e) Rotation mechanism of the rotors in the molecular ball bearing. Rotation takes place through alternate intramolecular ligand exchange and flip motion, both of which are accompanied by helix inversion between *M* and *P* forms. TS: transition state.

for H^c and H^d in the ^{1}H NMR spectrum of the resulting complex as a result of the formation of a sandwich-shaped structure (Figure 2b). The proton signals for the outer oxazoline rings, H^a and H^b, were shifted downfield, whereas those for the inner oxazoline rings, H^e and H^f, remained unchanged. This result suggests that the outer oxazoline rings selectively coordinate to Pt^{II} ions, a hypothesis that was also supported by the appearance of one of the H^c phenylene proton signals at $\delta = 10.3$ ppm; the significant downfield shift is due to the close position of this hydrogen atom to the Pt^{II} center. Electrospray ionization time-of-flight (ESI-TOF) mass spectrometry of a solution of the complex in CH$_3$OH showed three signals, at *m/z* 734.84, 955.76, and 1323.99, which can be assigned to $[\boldsymbol{Pt}_3\mathbf{3}_2\cdot(\mathrm{TfO})]^{5+}$, $[\boldsymbol{Pt}_3\mathbf{3}_2\cdot(\mathrm{TfO})_2]^{4+}$, and $[\boldsymbol{Pt}_3\mathbf{3}_2\cdot(\mathrm{TfO})_3]^{3+}$, respectively (see Figure S1 in the Supporting Information).

Finally, crystals suitable for X-ray crystallographic analysis of $[\boldsymbol{Pt}_3\mathbf{3}_2\cdot(\mathrm{TfO})_6]$ were obtained from a saturated solution of the complex in CH$_3$OH at room temperature after 2 days.[6] The crystal structure of the hexanuclear Pt^{II} complex clearly indicates that the complex has a sandwich-shaped helical structure, in which the outer oxazoline rings selectively coordinate to Pt^{II} ions, and the inner oxazoline rings are free to coordinate other ions (Figure 3a). The distance between the two disk-shaped ligands **3** is 12.0 Å, and therefore there is no structural correlation between them. All nitrogen atoms of the inner oxazoline rings face inward. This conformation appears not to be suitable for the correlation between the rotors in $[\mathrm{Ag}_6\boldsymbol{Pt}_3\mathbf{1}_2\cdot\mathbf{3}_2]^{12+}$ does not appear to be as significant as in $[\mathrm{Ag}_9\mathbf{1}_2\cdot\mathbf{3}_2]^{9+}$. In macroscopic devices, such machinery is known as a double ball bearing (Figure 1c), in which three rotors are aligned along a single rotation axis and can rotate independently.

The new rotor–transmitter–rotor, $[\mathrm{Ag}_6\boldsymbol{Pt}_3\mathbf{1}_2\cdot\mathbf{3}_2]^{12+}$, was constructed in a stepwise fashion: the central part, $[\boldsymbol{Pt}_3\mathbf{3}_2]^{6+}$, was built first, and then two rotors, **1**, were attached to both sides of the $[\boldsymbol{Pt}_3\mathbf{3}_2]^{6+}$ complex through the mediation of Ag^I ions. The central transmitter part, $[\boldsymbol{Pt}_3\mathbf{3}_2\cdot(\mathrm{TfO})_6]$, was formed quantitatively by mixing **3**, $\boldsymbol{Pt}\mathrm{Cl}_2$,[5] and AgOTf in dimethyl sulfoxide at 80 °C for 6 h. Two proton signals were observed

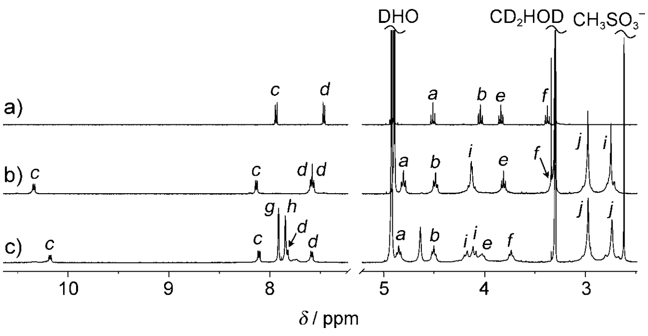

Figure 2. ^{1}H NMR spectra (500 MHz, CD$_3$OD, 293 K) of a) **3**, b) $[\boldsymbol{Pt}_3\mathbf{3}_2\cdot(\mathrm{TfO})_6]$, and c) $[\mathrm{Ag}_6\boldsymbol{Pt}_3\mathbf{1}_2\cdot\mathbf{3}_2\cdot(\mathrm{TfO})_6\cdot(\mathrm{MsO})_6]$.

© 2010 Wiley-VCH Verlag GmbH & Co. KGaA, Weinheim

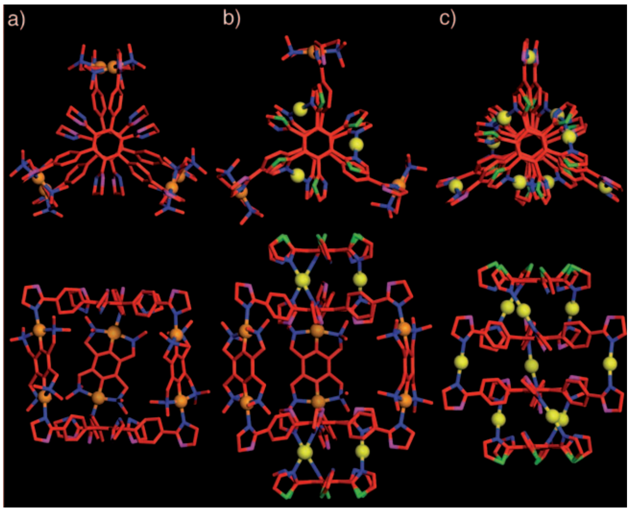

Figure 3. Crystal structures of a) [$\boldsymbol{Pt}_3\mathbf{3}_2$·(TfO)$_6$], b) [$Ag_6\boldsymbol{Pt}_3\mathbf{1}_2$·$\mathbf{3}_2$·(TfO)$_{12}$], and c) [$Ag_9\mathbf{1}_2$·$\mathbf{3}_2$·(TfO)$_9$] (C red, N blue, O purple, S green, Ag yellow, Pt brown). Hydrogen atoms and counteranions are omitted for clarity.

subsequent complexation to form the [$Ag_6\boldsymbol{Pt}_3\mathbf{1}_2$·$\mathbf{3}_2$]$^{12+}$ complex; however, this complex was eventually formed as a result of the low energy barrier to the rotation of the five-membered oxazoline rings in the hexasubstituted benzene derivatives.

The dodecanuclear Ag^{I}–Pt^{II} complex [$Ag_6\boldsymbol{Pt}_3\mathbf{1}_2$·$\mathbf{3}_2$]$^{12+}$ was formed by adding a solution of AgOMs (MsO$^-$: $CH_3SO_3^-$) and **1** (1:3) in CD_3OD to a solution of [$\boldsymbol{Pt}_3\mathbf{3}_2$·(TfO)$_6$] in CD_3OD (Figure 2c). The solubility of the Ag^{I}–Pt^{II} complex varies with the counteranion. When all the counteranions of the complex were TfO$^-$, the resulting complex precipitated in CD_3OD. On the other hand, when MsO$^-$ was used as the counteranion, the complex became soluble in CD_3OD, but the yield was not quantitative. Therefore, we examined a mixture of counteranions, TfO$^-$ and MsO$^-$. Upon the complexation of [$\boldsymbol{Pt}_3\mathbf{3}_2$·(TfO)$_6$] with AgOMs and **1** in CD_3OD, the complex [$Ag_6\boldsymbol{Pt}_3\mathbf{1}_2$·$\mathbf{3}_2$·(TfO)$_6$·(MsO)$_6$] was formed nearly quantitatively, as demonstrated by ^{1}H NMR spectroscopy (Figure 2c). The complex was also characterized by ESI-TOF mass spectrometry (see Figure S2 in the Supporting Information). Since the complex includes two kinds of counteranions, a number of signals were observed that were assignable to [$Ag_6\boldsymbol{Pt}_3\mathbf{1}_2$·$\mathbf{3}_2$·(TfO)$_m$·(MsO)$_n$]$^{(12-n-m)+}$.

The molecular structure of the Ag^{I}–Pt^{II} complex was revealed by X-ray crystallographic analysis (Figure 3b). Crystals suitable for single-crystal X-ray analysis were obtained by the diffusion of Et_2O into a solution of the complex in CH_3OH at 5 °C for 3 days.[7] The complex is 2.5 nm long along a coaxis of the four ligands, which are stacked to form a quadruple-decker structure in such a way that the central [$\boldsymbol{Pt}_3\mathbf{3}_2$]$^{6+}$ complex is positioned between the two terminal rotors **1** through Ag^{I} coordination. All Ag^{I} ions in the complex adopt a linear two-coordinate geometry, as was observed in the [$Ag_9\mathbf{1}_2$·$\mathbf{3}_2$·(TfO)$_9$] complex (Figure 3c).[4] Although the [$Ag_9\mathbf{1}_2$·$\mathbf{3}_2$]$^{9+}$ complex and its precursory [$\boldsymbol{Pt}_3\mathbf{3}_2$]$^{6+}$ complex have a helical structure, the [$Ag_6\boldsymbol{Pt}_3\mathbf{1}_2$·$\mathbf{3}_2$]$^{12+}$ complex has a mirror plane perpendicular to the rotational axis, and therefore the helix senses of the upper and lower ball-bearing units, [$Ag_3\mathbf{1}$·$\mathbf{3}$]$^{3+}$, are opposite to each other. One of the most significant features of the complex is that the ligand **3** located in the middle of the structure is notably bent (Figure 3b), whereas the ligand **3** of the precursory [$\boldsymbol{Pt}_3\mathbf{3}_2$]$^{6+}$ complex is flat (Figure 3a). In light of the fact that the [$Ag_9\mathbf{1}_2$·$\mathbf{3}_2$·(TfO)$_9$] complex shows the same tendency (Figure 3c), the Ag^{I}-mediated binding of the two rotors to the transmitter must cause the bending of **3**.

We previously reported a good method to assess motional correlation in the rotor–transmitter–rotors.[4] The method is indirect, but is the only practical method that overcomes the difficulties in evaluating the correlation between two chemically equivalent rotors. Since the rotation of the rotor **1** induces helix inversion through the rings in both the rotors and the inner rings of the transmitter, if the motions in the molecule are strongly correlated, the helix inversion of all the rings should take place at an identical rate. The rates of helix inversion of all the rings can be determined by analyzing the chemical exchange between geminal hydrogen atoms in both the inner and outer oxazoline rings. Because the inner oxazoline rings bind to the rotors **1** through Ag^{I} ions, the rates of helix inversion of the rotors can be determined by analyzing the H^e and H^f proton signals. Similarly, the rates of helix inversion of the remaining outer oxazoline rings in the transmitter can be obtained directly by analyzing the H^a and H^b proton signals. As for the [$Ag_9\mathbf{1}_2$·$\mathbf{3}_2$]$^{9+}$ complex, in which the four ligands are structurally correlated with each other, the rates of helix inversion of both the inner and the outer oxazoline rings were identical, which suggests strong correlation of their motion.[4] To investigate helix inversion in the [$Ag_6\boldsymbol{Pt}_3\mathbf{1}_2$·$\mathbf{3}_2$]$^{12+}$ complex, we conducted a VT ^{1}H NMR experiment. As the temperature was decreased, the signals for the geminal hydrogen atoms in both the inner and the outer oxazoline rings were separated as a result of the slow helix inversion of the oxazoline rings on the NMR timescale (Figure 4). In contrast, in a VT ^{1}H NMR experiment on the [$\boldsymbol{Pt}_3\mathbf{3}_2$]$^{6+}$ complex, the geminal hydrogen atoms were observed to be equivalent even at 213 K (see Figure S4 in the Supporting Information). This result indicates that the rates of helix inversion of both the inner and the outer oxazoline rings are affected by the connection of the terminal rotors **1** to the central [$\boldsymbol{Pt}_3\mathbf{3}_2$]$^{6+}$ complex through Ag^{I} coordination.

To evaluate the rate of chemical exchanges in the [$Ag_6\boldsymbol{Pt}_3\mathbf{1}_2$·$\mathbf{3}_2$]$^{12+}$ complex at each temperature, we conducted line-shape analysis of the proton signals H^a and H^f. However, it was hard to fit the data to the theory owing to the broadening and overlapping of the signals and to the appearance of unidentified signals at low temperatures. Therefore, we roughly estimated the rates of helix inversion of both types of oxazoline ring at the coalescence temperature by using the following equation: $k_c = \pi\Delta\delta/2^{1/2}$ (k_c: rate at the coalescence temperature [s^{-1}]; $\Delta\delta$: separation of the two chemically exchangeable protons [Hz]). The coalescence temperatures for H^a and H^f were estimated to be around 253 K. The rates of helix inversion of the inner and outer oxazoline rings at 253 K (k_{253}) were determined to be 4.3×10^2 and 1.5×10^2 s^{-1}, respectively. These values are much larger than the rate of helix inversion in the [$Ag_9\mathbf{1}_2$·$\mathbf{3}_2$]$^{9+}$ complex

© 2010 Wiley-VCH Verlag GmbH & Co. KGaA, Weinheim

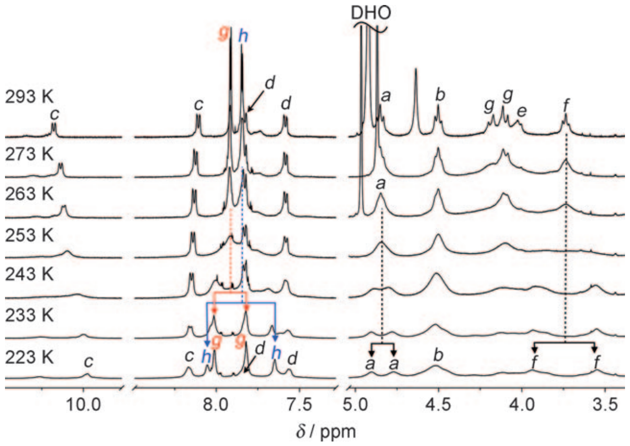

Figure 4. Variable-temperature ^{1}H NMR spectra (500 MHz, CD_3OD, 223–293 K) of $[Ag_6\boldsymbol{Pt}_3\mathbf{1}_2\cdot\mathbf{3}_2\cdot(TfO)_6\cdot(MsO)_6]$.

($k_{253} = 28\ s^{-1}$). This result is consistent with a lesser degree of interlocking between the two ligands **3** in the central $[\boldsymbol{Pt}_3\mathbf{3}_2]^{6+}$ complex, in which they are positioned 10.5 Å apart from each other. Given that the rates of helix inversion in both the rotor **1** and the inner oxazoline rings of **3** are three times higher than the rate of helix inversion in the outer oxazoline rings of **3**, it is apparent that the poorer correlation in motion of the transmitter, $[\boldsymbol{Pt}_3\mathbf{3}_2]^{6+}$, is due to the weaker structural link. In contrast, in the $[Ag_9\mathbf{1}_2\cdot\mathbf{3}_2]^{9+}$ complex, the ligands in the $[Ag_3\mathbf{3}_2]^{3+}$ transmitter are closely interlocked through helix inversion, and therefore the correlation in motion is strong between the two terminal rotors. Thus, the $[Ag_6\boldsymbol{Pt}_3\mathbf{1}_2\cdot\mathbf{3}_2]^{12+}$ complex behaves like a double ball bearing (Figure 1c), in which three rotational parts can move nearly independently of one another.

Since the two ligands **3** in the $[Ag_6\boldsymbol{Pt}_3\mathbf{1}_2\cdot\mathbf{3}_2]^{12+}$ complex are distant from one another, it was assumed that the rate of rotation of the rotors in the $[Ag_6\boldsymbol{Pt}_3\mathbf{1}_2\cdot\mathbf{3}_2]^{12+}$ complex would be similar to that observed for the ball bearing $[Ag_3\mathbf{1}\cdot\mathbf{2}]^{3+}$, and much faster than that observed for the $[Ag_9\mathbf{1}_2\cdot\mathbf{3}_2]^{9+}$ complex. We analyzed the intramolecular ligand exchange (see Figure 1e for $[Ag_3\mathbf{1}\cdot\mathbf{2}]^{3+}$) that takes place in the rotor **1** in the $[Ag_6\boldsymbol{Pt}_3\mathbf{1}_2\cdot\mathbf{3}_2]^{12+}$ complex from the chemical exchange of the hydrogen atoms H^g and H^h. At 293 K, one set of signals for H^g and H^h was observed (Figure 4), which indicated that the intramolecular ligand exchange was fast on the NMR timescale. When the temperature was decreased, each signal was separated into two signals with an identical integral value, which were assigned by an H–H COSY experiment at 223 K (see Figure S3 in the Supporting Information).[8] However, these signals overlapped with other proton signals for the complex and unidentified species that appeared at low temperatures. The rate of the intramolecular ligand exchange at the coalescence temperature around 253 K was thus estimated to be $k_{253} = 4.5\times10^2\ s^{-1}$, which is one order of magnitude faster than that observed for the rotor–transmitter–rotor $[Ag_9\mathbf{1}_2\cdot\mathbf{3}_2]^{9+}$, and slower than that observed for the molecular ball bearing $[Ag_3\mathbf{1}\cdot\mathbf{2}]^{3+}$.[9] These results reflect the degree of interlocking in these complexes. Given that the rate of intramolecular ligand exchange in the $[Ag_6\boldsymbol{Pt}_3\mathbf{1}_2\cdot\mathbf{3}_2]^{12+}$ complex is slower than that in $[Ag_3\mathbf{1}\cdot\mathbf{2}]^{3+}$, the three central $\boldsymbol{Pt}^{2+}$ complexes bridging the two terminal ball bearing units $[Ag_3\mathbf{1}\cdot\mathbf{3}]^{3+}$ appear to affect not only the rate of rotation, but also, to a certain extent, motional correlation.

In conclusion, an Ag^{I}–Pt^{II} dodecanuclear molecular rotational machinery, $[Ag_6\boldsymbol{Pt}_3\mathbf{1}_2\cdot\mathbf{3}_2]^{12+}$, with three rotational parts, was constructed in a two-step manner. Since the ligands **3** in the central connecting part, $[\boldsymbol{Pt}_3\mathbf{3}_2]^{6+}$, are positioned approximately 1.0 nm apart from each other, their motions are nearly independent. A comparison of the crystal structures of $[Ag_6\boldsymbol{Pt}_3\mathbf{1}_2\cdot\mathbf{3}_2]^{12+}$ and $[\boldsymbol{Pt}_3\mathbf{3}_2]^{6+}$ revealed that the $[\boldsymbol{Pt}_3\mathbf{3}_2]^{6+}$ unit in $[Ag_6\boldsymbol{Pt}_3\mathbf{1}_2\cdot\mathbf{3}_2]^{12+}$ has a *meso* structure, whereas the structure of $[\boldsymbol{Pt}_3\mathbf{3}_2]^{6+}$ itself has a screw sense (Figure 3a). Furthermore, the ligands **3** in $[Ag_6\boldsymbol{Pt}_3\mathbf{1}_2\cdot\mathbf{3}_2]^{12+}$ are bent, whereas those in $[\boldsymbol{Pt}_3\mathbf{3}_2]^{6+}$ are flat. These structural differences significantly affect the rate of rotation as well as the degree of correlation between the remote rotational motions. As a consequence, the $[Ag_6\boldsymbol{Pt}_3\mathbf{1}_2\cdot\mathbf{3}_2]^{12+}$ complex was found to behave like a double ball bearing in which three rotors that are coaxially arranged move independently of one another. The development of on–off control of the correlation in motion in multirotor systems is currently underway.

Received: October 22, 2009
Published online: January 29, 2010

Keywords: molecular devices · N ligands · platinum · silver · supramolecular chemistry

---

[1] For examples, see: a) G. S. Kottas, L. I. Clarke, D. Horinek, J. Michl, *Chem. Rev.* **2005**, *105*, 1281; b) K. Tashiro, K. Konishi, T. Aida, *J. Am. Chem. Soc.* **2000**, *122*, 7921; c) M. Ikeda, M. Takeuchi, S. Shinkai, F. Tani, Y. Naruta, S. Sakamoto, K. Yamaguchi, *Chem. Eur. J.* **2002**, *8*, 5541; d) M. F. Hawthorne, J. I. Zink, J. M. Skelton, M. J. Bayer, C. Liu, E. Livshits, R. Baer, D. Neuhauser, *Science* **2004**, *303*, 1849; e) T. Muraoka, K. Kinbara, T. Aida, *Nature* **2006**, *440*, 512; f) M. C. Jiménez, C. Dietrich-Buchecker, J.-P. Sauvage, *Angew. Chem.* **2000**, *112*, 3422; *Angew. Chem. Int. Ed.* **2000**, *39*, 3284; g) A. M. Stevens, C. J. Richards, *Tetrahedron Lett.* **1997**, *38*, 7805; h) G. Vives, A. Carella, J.-P. Launay, G. Rapenne, *Chem. Commun.* **2006**, 2283; i) H. J. Yoon, J. Heo, C. A. Mirkin, *J. Am. Chem. Soc.* **2007**, *129*, 14182; j) D. Braga, M. Curzi, A. Johansson, M. Polito, K. Rubini, F. Grepioni, *Angew. Chem.* **2006**, *118*, 148; *Angew. Chem. Int. Ed.* **2006**, *45*, 142; k) K.-J. Lin, S.-L. Fu, C.-Y. Cheng, W.-H. Chen, H.-M. Kao, *Angew. Chem.* **2004**, *116*, 4282; *Angew. Chem. Int. Ed.* **2004**, *43*, 4186.

[2] a) V. Balzani, M. Venturi, A. Credi, *Molecular Devices and Machines: A Journey into the Nanoworld*, 2nd ed., Wiley-VCH, Weinheim, **2008**; b) V. Balzani, A. Credi, F. M. Raymo, J. F. Stoddart, *Angew. Chem.* **2000**, *112*, 3484; *Angew. Chem. Int. Ed.* **2000**, *39*, 3348; c) E. R. Kay, D. A. Leigh, F. Zebetto, *Angew. Chem.* **2007**, *119*, 72; *Angew. Chem. Int. Ed.* **2007**, *46*, 72; d) S. Bonnet, J.-P. Collin, M. Koizumi, P. Mobian, J.-P. Sauvage, *Adv. Mater.* **2006**, *18*, 1239; e) Special Issue "Molecular Machines": *Acc. Chem. Res.* **2001**, *32*, 409; f) B. L. Feringa, *J. Org. Chem.* **2007**, *72*, 6635.

[3] a) S. Hiraoka, M. Shiro, M. Shionoya, *J. Am. Chem. Soc.* **2004**, *126*, 1214; b) S. Hiraoka, K. Hirata, M. Shionoya, *Angew. Chem.* **2004**, *116*, 3902; *Angew. Chem. Int. Ed.* **2004**, *43*, 3814.

[4] S. Hiraoka, E. Okuno, M. Shiro, M. Shionoya, *J. Am. Chem. Soc.* **2008**, *130*, 9089.

© 2010 Wiley-VCH Verlag GmbH & Co. KGaA, Weinheim

[5] P. Steenwinkel, H. Kooijman, W. J. J. Smeets, A. L. Spek, D. M. Grove, G. van Koten, *Organometallics* **1998**, *17*, 5411.

[6] Crystallographic data for $[\boldsymbol{Pt}_3\mathbf{3}_2\cdot(\mathrm{TfO})_6\cdot(\mathrm{CH_3OH})_6\cdot(\mathrm{H_2O})_{30}]$: colorless, $\mathrm{C_{150}H_{252}F_{18}N_{24}O_{66}Pt_6S_6}$, $M = 5152.63$, $T = 93.1$ K, block, $R32$, $Z = 3$, $a = b = 19.4486(7)$, $c = 53.926(4)$ Å, $\alpha = \beta = 90$, $\gamma = 120°$, $V = 17\,664.9(15)$ Å^3, $R = 0.0614$, $wR = 0.1729$, GOF = 1.036. CCDC 748365 contains the supplementary crystallographic data for this paper. These data can be obtained free of charge from The Cambridge Crystallographic Data Centre via www.ccdc.cam.ac.uk/data_request/cif.

[7] Crystallographic data for $[\mathrm{Ag}_6\boldsymbol{Pt}_3\mathbf{1}_2\cdot\mathbf{3}_2\cdot(\mathrm{TfO})_{12}\cdot(\mathrm{CH_3OH})_4\cdot(\mathrm{H_2O})_5]$: colorless, $\mathrm{C_{202}H_{218}Ag_6F_{36}N_{36}O_{57}Pt_6S_{24}}$, $M = 7333.28$, $T = 93.1$ K, block, $P6_3/m$, $Z = 2$, $a = b = 23.5632(5)$, $c = 28.2512(12)$ Å, $\alpha = \beta = 90$, $\gamma = 120°$, $V = 13\,584.3(10)$ Å^3, $R = 0.0954$, $wR = 0.3014$, GOF = 1.440. CCDC 748366 contains the supplementary crystallographic data for this paper. These data can be obtained free of charge from The Cambridge Crystallographic Data Centre via www.ccdc.cam.ac.uk/data_request/cif.

[8] The cooling of the solution of $[\mathrm{Ag}_6\boldsymbol{Pt}_3\mathbf{1}_2\cdot\mathbf{3}_2]^{12+}$ in $\mathrm{CD_3OD}$ led to a large upfield shift of one of the phenylene proton signals $\mathrm{H^c}$ (by $\delta = 0.5$ ppm). A similar shift was observed for the $[\boldsymbol{Pt}_3\mathbf{3}_2]^{6+}$ complex (see Figure S4 in the Supporting Information). This upfield shift is probably due to a conformation change in the $[\boldsymbol{Pt}_3\mathbf{3}_2]^{6+}$ unit, which keeps the hydrogen atom away from the $\mathrm{Pt^{II}}$ center.

[9] Given that the rate of helix inversion, k_{helix}, is the sum of the rates of intramolecular ligand exchange, k_{ex}, and flip motion, k_{flip}, k_{ex} should be smaller than k_{helix}. However, k_{ex} for $[\mathrm{Ag}_6\boldsymbol{Pt}_3\mathbf{1}_2\cdot\mathbf{3}_2]^{12+}$ is comparable to k_{helix}; therefore, k_{flip} should be rather small, as the rotation is slow on the NMR timescale. This conclusion is inconsistent with the observation for a similar $\mathrm{Ag^I}$–$\mathrm{Pt^{II}}$ dodecanuclear complex that has different rotors with C_1 symmetry that both the intramolecular ligand exchange and the flip motion are fast on the NMR timescale at 293 K. Furthermore, intermolecular ligand exchange between the rotors of different molecular ball bearings is very slow on the NMR timescale, as was demonstrated unambiguously by ^{1}H NMR and 2D EXSY experiments on a mixture of two different molecular ball bearings (see Figure S6 in the Supporting Information). We propose on the basis of these results that the rotors frequently change their relative positions through "slippage", without inversion of the helicity.

© 2010 Wiley-VCH Verlag GmbH & Co. KGaA, Weinheim